

Who Evaluates the Evaluations? Objectively Scoring Text-to-Image Prompt Coherence Metrics with T2IScoreScore (TS2)

Michael Saxon[⊗][Ⓜ] Fatima Jahara[⊗][Ⓜ] Mahsa Khoshnoodi[⊗][Ⓜ]
 Yujie Lu[⊗] Aditya Sharma[⊗] William Yang Wang[⊗]

[Ⓜ]University of California, Santa Barbara [Ⓜ]Fatima Al-Fihri Predoctoral Fellowship
[⊗]Equal contribution [Ⓜ]Contact: saxon@ucsb.edu

T2IScoreScore.github.io

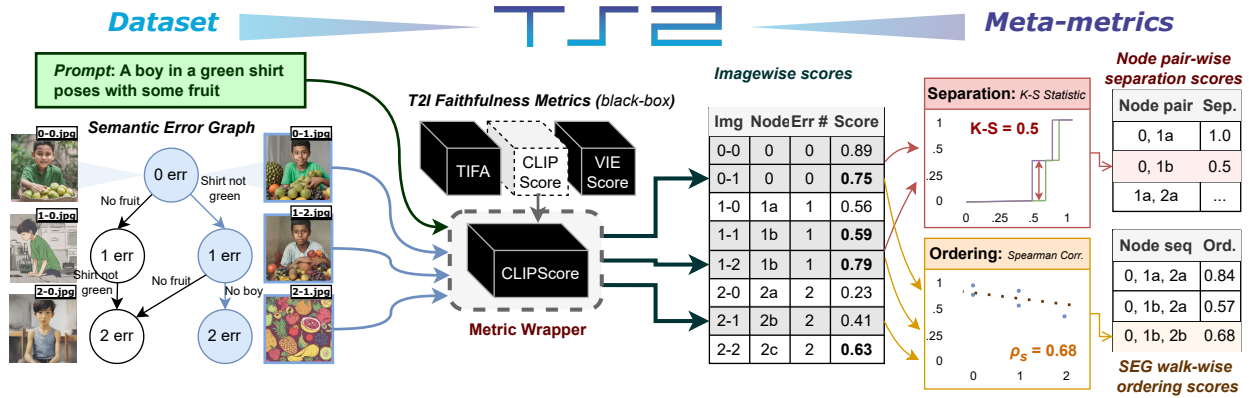


Figure 1: Overview of **T2IScoreScore**. T2I evaluation metrics are scored based on their ability to correctly organize images in a *semantic error graph* (SEG) relative to their generating prompt, checking ordering (Spearman’s ρ) and separation of nodes (Kolmogorov–Smirnov statistic).

Abstract

With advances in the quality of text-to-image (T2I) models has come interest in benchmarking their *prompt faithfulness*—the semantic coherence of generated images to the prompts they were conditioned on. A variety of T2I faithfulness metrics have been proposed, leveraging advances in cross-modal embeddings and vision-language models (VLMs). However, these metrics are not rigorously compared and benchmarked, instead presented against few weak baselines by correlation to human Likert scores over a set of easy-to-discriminate images.

We introduce **T2IScoreScore (TS2)**, a curated set of *semantic error graphs* containing a prompt and a set increasingly erroneous images. These allow us to rigorously judge whether a given prompt faithfulness metric can correctly order images with respect to their objective error count and significantly discriminate between different error nodes, using meta-metric scores derived from established statistical tests. Surprisingly, we find that the state-of-the-art VLM-based metrics (e.g., TIFA, DSG, LLMscore, VIEScore) we tested fail to significantly outperform simple feature-based metrics like CLIPScore, particularly on a hard subset of naturally-occurring T2I model errors. **TS2** will enable the development of better T2I prompt faithfulness metrics through more rigorous comparison of their conformity to expected orderings and separations under objective criteria.

1 Introduction

Text-to-image (T2I) models are improving at a breakneck pace in terms of quality, fidelity, and coherence of generated images to their conditioning prompts [39–42]. Despite this, persistent challenges in achieving image-prompt faithfulness [34, 6] remain—particularly in freely available models that don’t sit behind proprietary APIs. Indeed, many techniques to improve T2I models have been proposed of late, aiming to reduce hallucination [51, 9], duplication [25], and composition errors [9, 29], and missing objects [55, 10]. However, there is no consensus on how to best compare these many models and methods, so it is hard to objectively track T2I progress [43, 21].

A variety of automated *image-prompt coherence metrics* have been proposed, which rate the *faithfulness* of generated images, defined as the degree to which they satisfy the implicit requirements set forth in the generating prompt [11, 13, 30, 20]. These proposed metrics vary considerably in design; as rating how well an image matches to its prompt is a nontrivial multimodal challenge [21, 8, 22].

This variety itself presents a *meta-evaluation problem*: there is no consensus on how these faithfulness metrics ought to be compared, and consequently each new metric is validated on its own ad-hoc test set against prior baselines. Typically these *self-evaluations* consist of a set of prompt-image pairs with accompanying human annotations (usually simple Likert scores [8, 13]), and metrics are judged on their correlation to these human judgements [22].

Such self-evaluation is not ideal; authors may unwittingly tilt the scales by using evaluation examples which cater to the particular strengths of their proposed method, and variance of metric performance between different evaluation sets (containing different images and prompt semantics [45, 31]) is high [58]. Additionally, relying on correlation to human judgements of small sets of images across different prompts is highly subjective [15, 32] and prone to including judgements of quality and style that are orthogonal to prompt coherence. As a community we need a consistent and objective evaluation for T2I prompt-coherence metrics to enable trustworthy comparison.

To this end we propose **T2IScoreScore (TS2)**, an objective *benchmark for benchmarks*, to resolve these issues. While it contains a similar number of images to previously proposed coherence metric evaluation sets, it contains fewer prompts. This high image-to-prompt ratio allows us to organize the images along *semantic error graphs* (Figure 1), where each edge corresponds to an error of the image to present some attribute, element, or relation described in the prompt. These semantic error graphs permit objective scoring of a metric through two questions:

1. Can a metric correctly **order** increasingly wrong images against their generating prompt as error counts go up? (*Ord.*)
2. Can a metric reliably **separate** sets of images based on a single prompt-relevant semantic difference? (*Sep.*)

We adapt Spearman’s correlation ρ [47] and the two-sample Kolmogorov–Smirnov statistic [19] respectively to answer these questions. We score a broad set of T2I faithfulness metrics along all semantic error graphs (SEGs) in **TS2**. We find some surprising results: despite their inferior performance in correlating to human preferences [13, 6, 20, 30], simple feature-space methods like CLIPScore [11] are actually quite performant in terms of objective correctness, comparable or even superior to the more complicated vision-language model (VLM)-based ones (section 6).

In light of these surprising results, we hope to see the T2I evaluation community adopt **TS2** to rigorously guide the further advancement of T2I prompt coherence metrics that preserve the interpretability and subjective human correlation benefits of more rigorous methods, but also can significantly outperform simple baselines on our objective test. To summarize, in this work:

- We formalize the task of objectively assessing T2I prompt coherence metrics by their ability to correctly order and separate image populations within semantic error graphs (SEGs).
- We present **T2IScoreScore (TS2)**, our evaluation for this task: a benchmark dataset of 165 objective SEGs and 2,840 images, and meta-metrics for ordering and separation in SEGs.
- We evaluate a broad and representative set of T2I faithfulness benchmarks using **TS2**, demonstrate how it identifies novel failure cases.
- Motivate how future T2I faithfulness metrics can be improved by treating **TS2** performance as an orthogonal consideration to human preference correlation.

Dataset	Num Prompts	Num Total Images	Img. per Prompt Min:Avg:Max	Max Tree Depth	Max Tree Width	Ad-hoc	Objective
ImagenHub T2I [21]	197	–	–	–	–	✓	–
TIFA v1.0 [13]	4k	–	–	–	–	✓	–
DrawBench [42]	200	–	–	–	–	–	–
DSG-1k [6]	1k	–	–	–	–	✓	–
T2I-CompBench [14]	6k	–	–	–	–	–	–
ABC-6K [9]	6.4k	–	–	–	–	–	–
Flickr8k [12]	40k	8k	1:1:1	1	5	–	–
Flickr30k [35]	155k	31k	1:1:1	1	5	–	–
MS COCO Captions [4]	1.5m	330k	1:1:1	1	5	–	–
SeeTRUE [52]	31k	31k	1:1:1	1	1	✓	–
Pick-a-Pic [18]	35k	1M	2:2:2 ¹	1	2	✓	–
T2IScoreScore	165	2.8k	4:17:76	5	5	–	✓

Table 1: Comparison of T2I metric evaluation benchmarks. The first group of benchmarks are *prompt-only*², while the second group provides images. *Ad-hoc* benchmarks were introduced alongside a specific metric, *objective* benchmarks assess metrics based on explicitly enumerated errors (eg. missing objects) rather than relatively arbitrary human preference ratings.

2 Related Work

Advancements in text-to-image evaluation metrics and benchmarks necessitate evaluation for these metrics to understand their capabilities comprehensively. We discuss examples of both here.

Text-to-Image Metrics and Benchmarks Several benchmarks for T2I evaluation only contain prompts. The ImagenHub dataset [21] is a benchmark for evaluating text-to-image (T2I) models using prompts, specifically designed for tasks like text-guided image generation. DrawBench [42] provides a detailed evaluation of T2I models by incorporating text prompts to probe semantic attributes like compositionality, cardinality, and spatial relations. TIFA v1.0 [13] selects text inputs from the COCO validation set, DrawBench, PartiPrompt [54], and PaintSkill [5], while T2I-ComBench [14] covers compositionality, attribute binding, object relationships, and complex compositions. Some other T2I evaluation benchmarks derived from captioning datasets—like Flickr 8k, Flickr 30k, and MSCOCO—focus on comparing metrics correlation to captions generated from natural images [12, 35, 4]. The ABC-6K and CC500 benchmarks [9] evaluate attribute binding for text-to-image models, but they only focus on color attributes. Pick-a-Pic [18] is designed for gathering human preferences from generated images, and can be used to compare metrics. It contains over 500k examples, each consisting of a prompt, two generated images, and a label indicating the preferred image, or if there is a tie where neither image is significantly favored. TIFA and DSG [6] are two prominent metric proposal papers that use ad-hoc evals. TIFA uses a collection of 160 new annotations on 800 images generated from 160 prompts in the TIFA v1.0 dataset. DSG collects per-item (text-image pair) for TIFA 160 prompts [13] and per-question human judgments for the full DSG-1k prompts. More details on specific metrics are in section 5. Other evaluation dimensions such as multilinguality [44, 46] and stereotype bias [3] have also been explored.

Evaluation for Text-to-Image Evaluation Metrics SeeTRUE [52] is—to our knowledge—the only other existing benchmark for meta-evaluating T2I metrics, though they only evaluate the TIFA metric on visual entailment. They focus on accuracy in detecting binary misalignments in test images rather than on ranking. While this is also objective this evaluation does not capture the score ranking itself, only visual-text entailment. Their set also involves a mix of machine and human-produced augmentations, including generative alternative erroneous prompts for images (compared to our approach of generating images that are erroneous relative to prompt). As a consequence, there exist corresponding sets of multiple prompts for some images and multiple images for some prompts, but metrics are not assessed specifically on their ability to differentiate between these related examples in SeeTRUE. To the best of our knowledge, our **T2IScoreScore** is the first meta-metric to comprehensively evaluate prompt-image coherence metrics for T2I.

¹Although this benchmark has multiple pairs of images per prompt, pair is separately annotated with one preference image. With no way to compare across sets, the effective number of images per prompt is 2.

²Though these benchmarks are primarily intended for directly evaluating T2I models alongside their proposed metric, they are usually also used for metric evaluation by having human annotators provide faithfulness Likert scores for each prompt/image pair separately over some models generating images for each prompt.

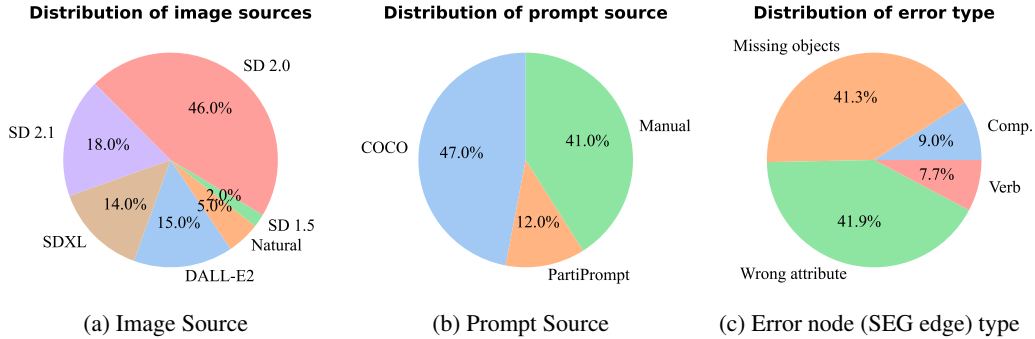


Figure 2: Overview of the distribution of sample types in **TS2**: (a) The source example images came from; 5% of images in the benchmark are real photographs from a stock image repository, while the remainder were generated by Stable Diffusion (SD) or DALL-E variants. (b) Source of the eliciting prompt; either existing resources or us (Manual). (c) Distribution of error types edges in all SEGs.

3 The T2IScoreScore Dataset

The goals of **TS2** are to determine whether a text-to-image model faithfulness scoring metric can correctly order a set of images of increasing incorrectness with respect to a prompt, and whether it can separate them within. We organize this evaluation based on *semantic error graphs* (SEGs), which contain one prompt and 4-76 images annotated with error node. We produce the SEGs using three different procedures, documented in [subsection 3.2](#).

3.1 Dataset Structure

TS2 contains 165 SEGs. Each SEG is based on a single prompt. Node “0” on each SEG contains at least one image that has been assessed by human annotators to contain no errors of verbal information (eg, entity in the image isn’t performing the described action), compositionality (eg, object described as “on top” but is beneath object), missing objects, or incorrect object attributes.

Each graph then contains a set of error nodes forming a directed acyclic graph. Each edge represents an error of one of the aforementioned types. Each node is labeled with the number of edges along its shortest path back to node 0, representing its error count ([Figure 1](#), [Figure 4](#)). Each node contains at least one image which is erroneous according to the described errors.

The images are sourced from a variety of text-to-image generation methods, including DALL-E 2 [40] Stable Diffusion 1.5 [41], 2.0, 2.1, and SDXL [36], and from natural repositories. The originating prompts are sourced from MS-COCO [26], PartiPrompt [54], and manually written by us. The proportion of image sources, prompt sources, and error types are documented in [Figure 2](#).

3.2 Dataset Collection Procedure

[Figure 3](#) depicts the three procedures by which we produce and populate SEGs with images, synthetic images from a synthetic graph (*Synth*), graph from natural images (*Nat*), and graph from real errors (*Real*). They are differentiated in terms of prompt sourcing, image sourcing, and the order in which those two steps are integrated with the graph.

Synth. The synthetic images are produced “graph first.” From an initial prompt sourced from one of the aforementioned prompt sources, we construct an error graph by first listing all entities and properties prescribed in the prompt, and then ablatively writing prompts where the elements are sequentially removed.

For example, in the left panel of [Figure 3](#), the initial prompt “a Christmas tree with lights and a teddy bear” is converted subtractively down to the prompt, “a Christmas tree with lights,” “a Christmas tree,” etc. Each of these prompts describes the error nodes where their respectively removed objects are missing. From the prompts representing each node we generate a set of images using one of our T2I models, and verify that each image is correct for its error node.

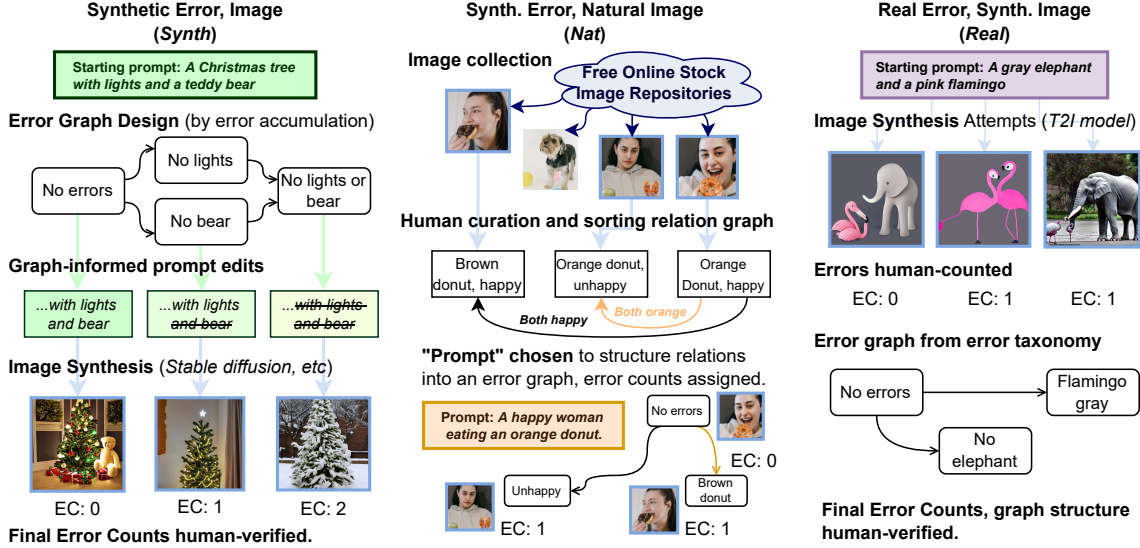


Figure 3: The three methods used to collect images to populate *semantic error graphs* with respect to the input prompts. **Synth.** (images generated from multiple prompts written to populate a SEG), **Nat.** (natural images populate a SEG), and **Real** (real errors from image generation attempts from one prompt populate a SEG).

Nat. The natural error trees exclusively contain real images sourced from the free stock image repository Pexels³. For this population, we follow an “image, graph, prompt” order. Multiple images with the same models, props, and scenes, with different arrangements from photoshoots are sourced. From these sets, we curate a relation graph describing the way in which the images differ in terms of objects, actions, attributes, and composition. We then select a head node based on centrality in this relation graph. Finally, a prompt is written to describe this head node with error count 0. An example is in the center panel of Figure 3.

We produced a set of natural image error graphs to assess whether distributional differences between synthetic images and real images might lead to measurable impacts on performance for the faithfulness metrics that typically use base models pretrained exclusively on natural images [38].

Real. The real error, synthetic image examples are following a “prompt, image, graph” order. From a starting prompt, either written by us or sourced from the aforementioned prompt sources, we use one of the T2I models to generate a set of images, exclusively using this starting prompt without modifications.

When we identify a prompt that causes some model to produce many images containing errors, we first count the amount of errors in each generated image, and draw the error graph between them to produce the final SEG. This procedure is documented in the right panel of Figure 3.

4 T2IScoreScore Meta-Metrics

A good prompt coherence metric should correctly reproduce the rank order of the semantic distance by scoring more distant images as less coherent than nearer ones (**ordering**) and should separate sets of images at different nodes (**separation**). We check both of these properties by comparing scores assigned by a metric to each semantic error graph (SEG)

For each SEG $S \in \text{SEGS}$ we introduce measures of a metric m : $\text{rank}_m(S)$ and $\text{sep}_m(S)$. Both of these measures are derived from well-established statistics, applied over every valid walk W of adjacent nodes N through graph S . The average of these rank and sep over all S represent the final **TS2** scores for a metric. For ease of notation, we refer to each SEG as a set of valid descending walks

³Available at <https://pexels.com>

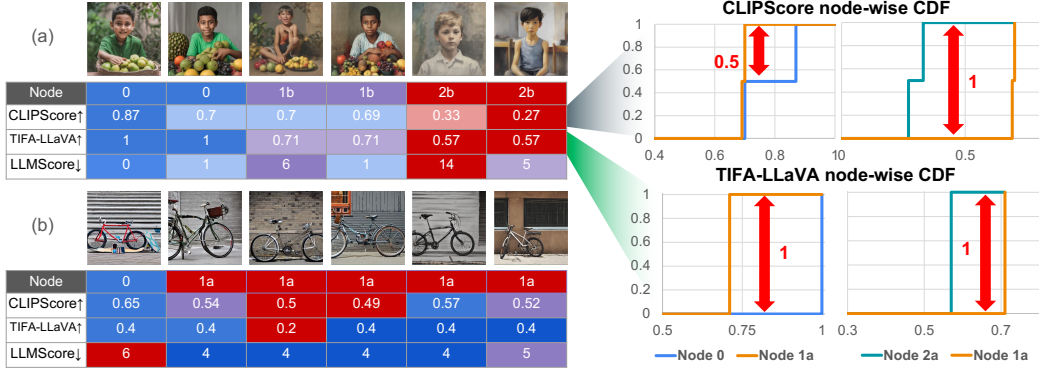


Figure 4: Examples of scores assigned by three metrics to examples from an easy (a) and hard (b) semantic error graph (left). Computation of the separation score $\text{sep}_m(S)$ for two metrics is depicted at the right. Color coding of each cell corresponds to the metric’s score for the image being better (blue) or worse (red); more correlated measures (presenting a higher rank order score $\text{rank}_m(S)$) will show the same progression from red to blue (a), while harder-to-rank examples will not (b).

$W \in S$ over nodes of increasing error count (eg, (0, 1a, 2a), (0, 1a, 2b), etc), where each walk defined as the in-order set of all (image, prompt, num. error) triples $(I, P, N) \in W$, even though each SEG contains only one prompt, and nodes may contain multiple images.

4.1 Ranking correctness assessment (Ordering)

We use Spearman’s rank correlation coefficient r_s [47] between image-level rank and metric-assigned score over every descending walk on the error accumulation tree to assess how well each metric correctly orders each image set. It is defined as the Pearson’s correlation of the rank orders $R(X)$, $R(Y)$ for sets X, Y :

$$r_s(X, Y) = \frac{\text{cov}(R(X), R(Y))}{\sigma_{R(X)}\sigma_{R(Y)}}; \quad R(X) = \left\{ \sum_{x_i \in X} \mathbb{1}(x_i < x) \mid x_i \in X \right\} \quad (1)$$

Thus, in our case the SEG-level rank order score $\text{rank}_m(S)$ is defined as:

$$\text{rank}_m(S) = \frac{1}{|S|} \sum_{W \in S} r_s(\{m(I, P) \mid (I, P, N) \in W\}, \{N \mid (I, P, N) \in W\}) \quad (2)$$

One limitation for using Spearman’s r for characterizing sets of scores is that it is undefined if one set $R(U)$ exclusively contains identical elements, as $\sigma_{R(U)} = 0$. For tractability in these scenarios we define $r_s(\cdot, U) := 0$, which is a reasonable definition to adopt, as if a metric assigns identical scores to all examples across different error levels, it presents no discernible relationship between error severity and score for that image set.

4.2 Assessing separation of error populations (Separation)

We assess the two-sample Kolmogorov–Smirnov statistic [19] pairwise between the populations of metric m ’s scores assigned to each sample between two error nodes n_i and n_j as populations. The Kolmogorov–Smirnov statistic is a non-parametric measure of the separation between two distributions [37, 2], defined as the maximum vertical difference between their empirical cumulative distribution functions $D_{KS}(X, Y)$:

$$D_{KS}(X, Y) = \sup_{x \in R_m} |F_X(x) - F_Y(x)| \quad (3)$$

Where $F_X(x)$ is proportion of samples in population X for which the metric value $m(i) \leq x$, (see Figure 4 for a visual depiction). We compute D_{KS} for every pair of adjacent error nodes in each tree walk W^4 , and report the average over all of these as the SEG separation score $\text{sep}_m(S)$:

$$\text{sep}_m(S) = \frac{1}{|S|} \sum_{N_i \in W} D_{KS}(\{m(P, I) | (P, I) \in N_i\}, \{m(P, I) | (P, I) \in N_{i+1}\}) \quad (4)$$

5 Experiments

Using **T2IScoreScore** we evaluated three kinds of T2I evaluation metrics: *embedding-based* (comparing embeddings within or across modalities), *caption-based* (comparing captions extracted from the generated images to the original prompt) *question-based* (using VQA or VLMs to answer generated questions from the prompt). Within these classes of metrics, we evaluated using multiple different multimodal LMs as backbones for question answering or captioning.

For each metric, we score every image in every SEG against its respective prompt. We report the results of our (section 4) Ordering and Separation metrics across all SEGs, as well as for our proposed subsets of SEGs.

5.1 Embedding-correlation Metrics

The first class of text-to-image scoring techniques we considered directly compare encodings of the prompt and image in a shared embedding space, using eg. cosine similarity.

CLIPScore [11] is a popular approach for comparing the faithfulness of a caption to an image (analogous to the task of comparing a synthetic image’s faithfulness to its prompt) and has consequently become popular for evaluating text-to-image models. CLIPScore is computed as the cosine similarity of the L_2 -normalized CLIP-assessed [38] image and text embeddings for CLIP model \mathcal{M} , for image i and prompt p :

$$\text{clip-s}(p, i) = \cos(\|\mathcal{M}_I(i)\|_2, \|\mathcal{M}_T(p)\|_2) \quad (5)$$

ALIGNScore (not to be confused with the text-only *AlignScore* [56]) is a variant embedding-based similarity score where we use the ALIGN [16] dual text-image embedding model from Kakao Brain to embed the prompt and image. It is computed equivalently to Equation 5, using `align-base` for model \mathcal{M} .

5.2 QG/A Metrics

Question Generation & Answering Metrics (QG/A) first use an LLM \mathcal{M}_{QG} to produce a set of requirement question/answer pairs $(q, a) \in Q$ from the prompt p , and then use a vision-language model \mathcal{M}_{VL} to check if each requirement has been satisfied, reporting the requirement satisfaction rate as the image’s faithfulness score relative to the prompt. Alternate realizations of this technique vary primarily in how questions are generated and how they relate to each other.

TIFA [13] prompts an LLM (eg, GPT-3) to generate a set of multiple choice and yes-no questions and their expected answers relative to the prompt. Then a vision language model \mathcal{M}_{VL} produces “free-form” answers to each question, which are converted into multiple choice answers a' using an SBERT model. The TIFA score for a given image is then the rate of correct answers,

$$\text{tifa-s}(p, i) = \frac{1}{|Q|} \sum_{(q, a) \in Q} \mathbb{1}(\mathcal{M}_B(\mathcal{M}_{VL}(i, q)) = a) \quad (6)$$

⁴We reformulate W to return nodes $N \in W$ containing pairs of prompt, image $(P, I) \in W$ to make this equation easier to read.

DSG (*Davidsonian scene graph*) [6] shares QA structure of TIFA, but generates a set of requirement questions which are non-overlapping, have exclusively yes/no answers, and sit on a directed acyclic graph such that a question is only satisfied if it and all its parent questions are answered *yes*.

5.3 Caption-comparison Metrics

The final class of metrics we consider use a two-tiered approach, first generating captions c of the generated images i using some captioning model \mathcal{M}_C , and then comparing the captions to the original prompt p using some LM \mathcal{M}_L .

LLMScore [30] captures the fine-grained similarity between the image and text with rationales by leveraging the visual details understanding capability from vision experts and the reasoning capability of LLMs. The visual information is parsed in hierarchical scene descriptions with global and local captions. Then the text-only LLMs will compare the multi-granularity visual descriptions with the input text prompt to give a score according to the evaluation guideline prompt.

VIEScore [20] rates aspects of semantic consistency (SC) and perceptual quality (PQ) ultimately providing a rating score on a scale of 0 and 10. We use 0-shot LLaVA-1.5 as the backbone MLLM to evaluate how successfully the image follows the text-to-image prompt.

5.4 Evaluating multiple backend VLMs

All QG/A and Caption-comparison metrics rely on the use of a generative vision-language model (VLM) either for performing question answering (\mathcal{M}_{VL} in subsection 5.2) or captioning (\mathcal{M}_C in subsection 5.3). Thanks to the simple decomposable framework of the QG/A methodologies, we were able to efficiently test the performance of both TIFA and DSG using five different VLMs as visual question-answering backends \mathcal{M}_{VL} . We tested:

mPLUG is a class of vision-language models that use skip connections between visual encoder embedding layers between cross-modal attention blocks in the transformer stack [23]. We use the mPLUG-OWL [53] 7b checkpoint which uses LLaMA 7b [49] as the pretrained text encoder.

LLaVA is a fine-tune of Vicuna [57] (decoder-only transformer model) that uses a learned MLP “vision-language connector” layer to map a single input image’s CLIP encodings into a shared embedding space [28, 27]. We use LLaVA 1.5 13b. Because LLaVA was instruction fine-tuned for chat applications, we experiment with a variant system prompt that requests *concise* answers from the system. We mark this alternate option LLaVa 1.5 (alt) in plots and figures.

BLIP is a jointly-trained self-attention ViT trained with cross attention to multiple transformer encoder and decoder pipelines with different tasks [24]. We use the BLIP encoder/causal LM decoder combination as a transformer encoder-decoder model to produce VQA answers from the `blip-vqa-base` checkpoint.

InstructBLIP extends BLIP by including an instruction fine-tuned “Q-Former” that selects salient instruction-related visual features from a frozen ViT for input to a frozen LLM that answers the query conditioned on the selected features [7]. We use `instructblip-flan-t5-xl`.

Fuyu is a decoder-only VLM that splits an input image into a sequence of patches that are separately projected directly into the transformer embedding space, which jointly learns ViT and LM behaviors [1]. We use `Fuyu-8b`.

6 Results

Table 2 shows the results for the Spearman Correlation **Ordering** feature rank_m and the K-S **Separation** feature sep_m for each metric we assessed, on average for all SEGs (Avg), and the three SEG subsets Synth, Nat, and Real.

		CLIPScore	ALIGNScore	mPLUG	LLaVA 1.5	LLaVA 1.5 (alt)	InstructBLIP	BLIP1	Fuyu	mPLUG	LLaVA 1.5	LLaVA 1.5 (alt)	InstructBLIP	BLIP1	Fuyu	LLMScore EC	LLMScore Over	VIEScore
		Emb-based			TIFA				DSG				Caption-based					
Ord.	Avg	71.4	73.9	71.0	74.5	74.4	76.5	73.8	38.7	70.4	76.2	75.0	79.0	76.6	29.5	48.8	57.7	37.8
	Synth	75.0	77.6	72.6	79.2	79.2	80.2	78.8	44.5	74.6	80.1	81.6	85.1	81.6	35.4	50.2	61.6	42.5
	Nat	58.0	70.2	66.9	62.8	64.0	65.1	62.2	23.5	65.3	65.9	68.8	70.7	71.6	20.5	36.2	44.4	22.4
	Real	69.3	62.6	68.2	66.7	64.5	71.6	64.0	29.7	58.4	70.0	54.2	62.0	61.2	14.2	54.4	54.1	33.2
Sep.	Avg	90.7	92.8	80.6	84.3	81.9	85.0	81.8	67.2	78.4	83.1	80.3	84.2	80.8	63.6	73.6	73.5	51.8
	Synth	90.5	94.1	80.6	87.5	85.2	86.7	84.1	67.3	80.9	85.7	83.9	87.8	84.9	65.8	71.1	72.8	53.7
	Nat	91.5	92.6	84.2	83.4	75.6	82.8	77.9	75.7	71.2	80.9	76.7	81.8	73.3	68.6	80.5	76.7	44.5
	Real	90.3	87.9	77.4	72.7	74.4	80.5	76.4	59.3	75.1	74.5	69.4	71.9	70.8	50.3	77.3	73.6	50.7

Table 2: Average Spearman Correlation rank_m (Ord.) and Kolmogorov–Smirnov separation score sep_m (Sep.) for each model (reported as % for readability). Best **bold**, within 2% of best *italic*, top three colored by metric type (emb-based, TIFA, DSG).

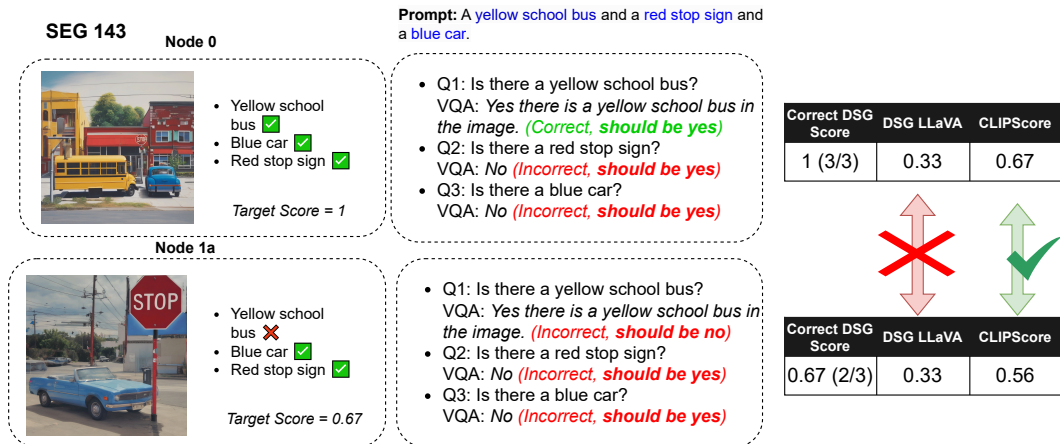


Figure 5: Example of two images on nodes 0 and 1 from a hard SEG that are correctly separated (and ranked) by CLIPScore but are not separated by DSG-LLaVA.

As we expected, we found that the Synth set consisting of hand-designed (and probably more obvious) errors was the easiest subset for all metrics to correctly order. The average rank_m score for Synth across all metrics was 70%, for Nat 55% and for Real 56%. However, different subsets were hard for different classes of metrics. For the Embedding-correlation and Caption-comparison metrics, Nat was the harder subset than Real. For the QG/A metrics, Real was harder.

As the embedding-based metrics are the original prompt faithfulness techniques proposed, TIFA [13], DSG [6], LLMScore [30], and VIEScore [20] all compare themselves against CLIPScore [11] in their introductory works. To our surprise, despite the commanding lead these metrics hold over LLMScore on their own ad-hoc evaluations, the simpler (and less computationally expensive) embedding-correlation metrics are competitive (or outperform) these VLM-based metrics (TIFA, DSG, caption-based), particularly on the hardest subsets.

In terms of separating the nodewise populations of image scores (Sep.), the embedding-based metrics are strictly better than the VLM-based ones.

6.1 Discussion

One disadvantage of using Spearman’s r is that it ‘expects’ ties to be the same in both distributions. For example, if a set of images has error count (0, 1, 1, 2), the ordering (1, 0.5, 0.5, 0) will have a perfect $r = 1$, while the ordering (1, 0.51, 0.49, 0) will be penalized, despite it also presenting a correct

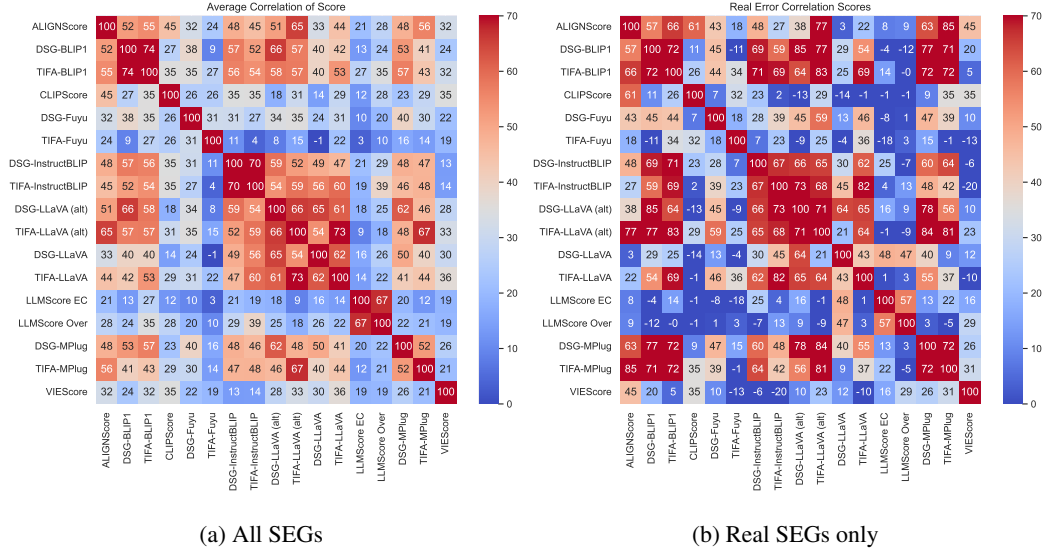


Figure 6: Correlation between the Spearman correlation score for each prompt tree for each metric, for all trees (a) and for the real error subset (b).

ordering. This means that **our Ordering score sep_m systematically punishes the embedding-based metrics relative to the VLM-based ones**, as the embedding-correlation metrics CLIPScore and ALIGNScore can take continuous values, while TIFA, DSG, LLMscore, and VIEScore have a discrete range. In light of this disparity the strong embedding metric performance is striking.

Another interesting weakness of the QG/A metrics is that many unlucky situations where the VLM backend presents a mix of true and false positives that cause incorrect rankings or poor separation (DSG fails to order samples while CLIPScore succeeds in Figure 5) to occur. However, these VLM failures cases are interpretable and can be targeted; **T2IScoreScore** will hopefully drive future work in making LMs more robust to these sorts of errors for VQA to mitigate this issue. In addition to these interpretability advantages, the more sophisticated VLM-based metrics still do present better subjective human preference correlation than CLIPScore [13, 6, 30, 20]. By focusing exclusively on objective similar-image ordering and separation, **TS2** is effectively orthogonal to these preference evals.

Given the documented biases LLMs have in directly outputting numbers [48, 33], it isn't a surprise that the technique which directly prompts VLMs to output a numerical preference value (VIEScore) is at present the least robust.

In general it seems that the most successful methods that leverage VLMs (TIFA and DSG) still ultimately produce scores using a deterministic algorithm. They use VLMs in a perceptual manner to separately check each requirement, but the final score is the accuracy estimate from each separate VQA question. This comports with the theories of LLM function that treat it as a "system 1" [50]; effectively TIFA and DSG are examples of *VLM-modulo* frameworks outperforming pure LLMs on the task of prompt coherence scoring [17].

Ultimately, all image coherence evaluation metrics stand to improve from further advances in general VLM quality. Due to rate limits at the time of submission, we couldn't feasibly assess the metrics using GPT4V as a backbone. As a considerably stronger model than LLaVA, mPLUG, etc, it is likely that the performance of the VLM-based metrics will be boosted when GPT4V is used.

Are the same SEGs hard for the same models? Figure 6 and Figure 7 present correlation plots between SEG-wise rank_m and sep_m scores respectively between each pair of metrics. For both we show (a) the correlations over all SEGs, and (b) the correlations between only SEGs in the Real subset. These plots show that broadly, similar methods have similar "blind spot" SEGs, while different ones can vary wildly in terms of which examples they succeed and fail at ordering and separating. Note that all TIFA or DSG QG/A metrics have appreciable correlation to each other, provided they use a strong enough VLM. The metrics employing weak VLMs such as Fuyu do not perform well. Similarly, the

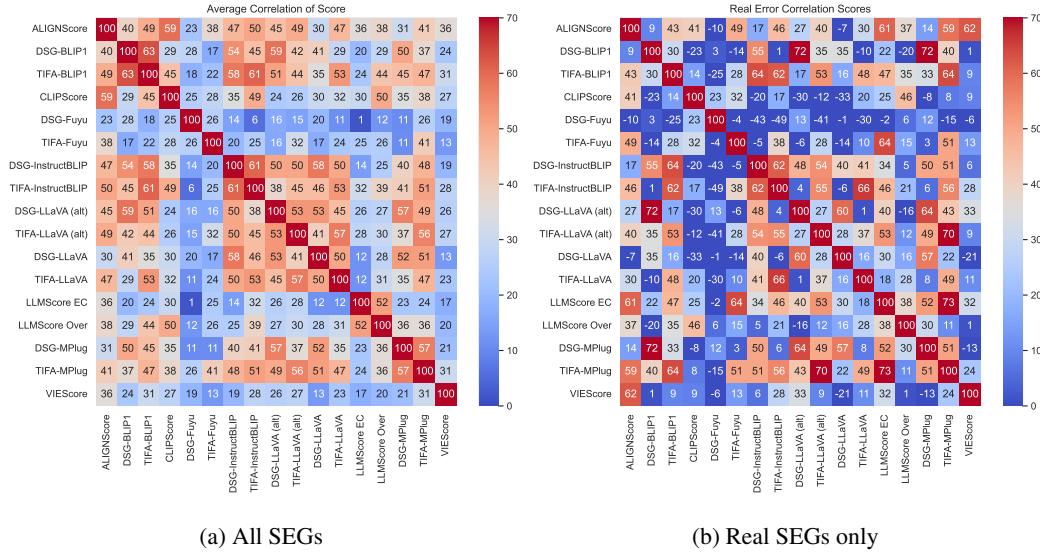


Figure 7: Correlation between the Kolmogorov-Smirnov statistic **Sep.** correlation score for each prompt tree for each metric, for all trees (a) and for the real error subset (b).

two LLMscore metrics are highly correlated to each other; the pure VLM numerical rating methods are not producing random noise. These correlations are stronger in the full set of SEGs (including natural images and the easy, pre-designed Synth SEGs) than they are in the hardest Real set of SEGs.

Although the scores of many models on our metric are high, this meta-evaluation is far from “solved.” In principle it should be possible to get much closer to 100 on average for both meta-metrics than we find. We view use of **TS2** as a necessary secondary evaluation for any new proposed T2I faithfulness metric; if it has high correlation to subjective human judgements but does not perform well here, skepticism might be warranted.

7 Conclusion

In conclusion, our investigation into the effectiveness of various text-to-image (T2I) prompt faithfulness metrics through the introduction of **T2IScoreScore**, a comprehensive dataset of semantic error graphs, reveals critical insights into the current state of evaluating T2I model performance. The relatively small number of prompts vs images (and consequent high image-prompt ratio) uniquely enables our meta-metrics to objectively analyze prompt-image coherence metrics, by assessing their ability to separate and order semantically different subpopulations relative to a specific prompt.

Despite the sophistication of vision-language models (VLMs) and other advanced metrics, our findings indicate that simpler feature-based metrics like CLIPScore still do perform comparably on this objective evaluation, especially when dealing with complex, naturally-occurring T2I model errors. This underscores the necessity for a more nuanced approach to benchmarking and developing metrics capable of capturing the subtle semantic nuances between prompts and generated images. The establishment of **T2IScoreScore** as a benchmarking tool is a significant step forward, offering a structured way to rigorously test and improve T2I prompt faithfulness metrics, ensuring they can more accurately reflect the semantic coherence between prompts and generated images, thereby facilitating the development of more reliable and effective T2I models.

Acknowledgements

We thank the organizers and sponsors of the Fatima Al-Fihri Predoctoral Fellowship program for compute resources. This work was supported in part by the National Science Foundation Graduate Research Fellowship under Grant No. 1650114, and CAREER Award under Grant No. 2048122.

Impact Statement

This research significantly contributes to steering text-to-image (T2I) generation technology in the right direction by addressing the critical need for precise evaluation of the semantic coherence between prompts and the generated images. The introduction of **T2IScoreScore**, with its semantic error graphs, offers a new benchmarking tool that not only tests the fidelity of T2I prompt faithfulness metrics but also sheds light on the comparative effectiveness of simpler versus more complex evaluation models. This nuanced understanding helps in refining the evaluation metrics, which is essential for guiding the development of T2I models towards generating images that are accurately aligned to their prompts.

Contribution Statement

MS checked a subset of the SEGs, designed the benchmark and meta-metrics, implemented the SEG tree iteration process and evaluation code for the Spearman Ordering and K-S Separation scores, collated the QG/A answers into ID-level scores, and assessed the final scores.

MK produced the Nat SEGs and produced, annotated, and checked a subset of the Real SEGs. MK generated the TIFA and DSG questions for all prompts, implemented and evaluated CLIPScore and ALIGNScore, collected answers for the QG/A metrics from BLIP, InstructBLIP, and refactored code.

FJ produced and annotated the Synth SEGs and produced, annotated, and checked a subset of the Real SEGs. FJ collected answers for Fuyu for the QG/A metrics and cleaned and organized the final dataset release.

YL evaluated LLMScore for the examples and conceived of measuring faithfulness errors in T2I faithfulness metrics. AS collected answers for the QG/A metrics from LLaVA and VIEScore.

References

- [1] R. Bavishi, E. Elsen, C. Hawthorne, M. Nye, A. Odena, A. Somani, and S. Taşlılar. Introducing our multimodal models (fuyu-8b), 2023. URL <https://www.adept.ai/blog/fuyu-8b>. 8
- [2] V. W. Berger and Y. Zhou. Kolmogorov–smirnov test: Overview. *Wiley statsref: Statistics reference online*, 2014. 6
- [3] F. Bianchi, P. Kalluri, E. Durmus, F. Ladhak, M. Cheng, D. Nozza, T. Hashimoto, D. Jurafsky, J. Zou, and A. Caliskan. Easily Accessible Text-to-Image Generation Amplifies Demographic Stereotypes at Large Scale. In *Proceedings of the 2023 ACM Conference on Fairness, Accountability, and Transparency*, FAccT '23, pages 1493–1504. Association for Computing Machinery. ISBN 9798400701924. doi: 10.1145/3593013.3594095. URL <https://dl.acm.org/doi/10.1145/3593013.3594095>. 3
- [4] X. Chen, H. Fang, T.-Y. Lin, R. Vedantam, S. Gupta, P. Dollar, and C. L. Zitnick. Microsoft coco captions: Data collection and evaluation server, 2015. 3
- [5] J. Cho, A. Zala, and M. Bansal. Dall-eval: Probing the reasoning skills and social biases of text-to-image generation models, 2023. 3
- [6] J. Cho, Y. Hu, R. Garg, P. Anderson, R. Krishna, J. Baldrige, M. Bansal, J. Pont-Tuset, and S. Wang. Davidsonian scene graph: Improving reliability in fine-grained evaluation for text-to-image generation, 2024. 2, 3, 8, 9, 10, 17
- [7] W. Dai, J. Li, D. Li, A. M. H. Tiong, J. Zhao, W. Wang, B. Li, P. Fung, and S. Hoi. Instructblip: Towards general-purpose vision-language models with instruction tuning, 2023. 8
- [8] E. L. Denton, S. Chintala, R. Fergus, et al. Deep generative image models using a laplacian pyramid of adversarial networks. *Advances in neural information processing systems*, 28, 2015. 2
- [9] W. Feng, X. He, T.-J. Fu, V. Jampani, A. Akula, P. Narayana, S. Basu, X. E. Wang, and W. Y. Wang. Training-free structured diffusion guidance for compositional text-to-image synthesis. *arXiv preprint arXiv:2212.05032*, 2022. 2, 3

- [10] W. Feng, W. Zhu, T.-j. Fu, V. Jampani, A. Akula, X. He, S. Basu, X. E. Wang, and W. Y. Wang. Layoutgpt: Compositional visual planning and generation with large language models. *Advances in Neural Information Processing Systems*, 36, 2024. 2
- [11] J. Hessel, A. Holtzman, M. Forbes, R. Le Bras, and Y. Choi. Clipscore: A reference-free evaluation metric for image captioning. In *Proceedings of the 2021 Conference on Empirical Methods in Natural Language Processing*, pages 7514–7528, 2021. 2, 7, 9
- [12] M. Hodosh, P. Young, and J. Hockenmaier. Framing image description as a ranking task: Data, models and evaluation metrics. In M. Wooldridge and Q. Yang, editors, *IJCAI 2015 - Proceedings of the 24th International Joint Conference on Artificial Intelligence*, IJCAI International Joint Conference on Artificial Intelligence, pages 4188–4192. International Joint Conferences on Artificial Intelligence, 2015. 24th International Joint Conference on Artificial Intelligence, IJCAI 2015 ; Conference date: 25-07-2015 Through 31-07-2015. 3
- [13] Y. Hu, B. Liu, J. Kasai, Y. Wang, M. Ostendorf, R. Krishna, and N. A. Smith. TIFA: Accurate and Interpretable Text-to-Image Faithfulness Evaluation with Question Answering. URL <http://arxiv.org/abs/2303.11897>. 2, 3, 7, 9, 10, 17
- [14] K. Huang, K. Sun, E. Xie, Z. Li, and X. Liu. T2i-compbench: A comprehensive benchmark for open-world compositional text-to-image generation, 2023. 3
- [15] P. Isola, J.-Y. Zhu, T. Zhou, and A. A. Efros. Image-to-image translation with conditional adversarial networks. In *Proceedings of the IEEE conference on computer vision and pattern recognition*, pages 1125–1134, 2017. 2
- [16] C. Jia, Y. Yang, Y. Xia, Y.-T. Chen, Z. Parekh, H. Pham, Q. Le, Y.-H. Sung, Z. Li, and T. Duerig. Scaling up visual and vision-language representation learning with noisy text supervision. In *International conference on machine learning*, pages 4904–4916. PMLR, 2021. 7
- [17] S. Kambhampati, K. Valmeekam, L. Guan, K. Stechly, M. Verma, S. Bhambri, L. Saldyt, and A. Murthy. Llms can’t plan, but can help planning in llm-modulo frameworks. *arXiv preprint arXiv:2402.01817*, 2024. 10
- [18] Y. Kirstain, A. Polyak, U. Singer, S. Matiana, J. Penna, and O. Levy. Pick-a-pic: An open dataset of user preferences for text-to-image generation. *Advances in Neural Information Processing Systems*, 36, 2024. 3
- [19] A. N. Kolmogorov. Sulla determinazione empirica di una legge di distribuzione. *Giorn Dell’inst Ital Degli Att*, 4:89–91, 1933. 2, 6
- [20] M. Ku, D. Jiang, C. Wei, X. Yue, and W. Chen. Viescore: Towards explainable metrics for conditional image synthesis evaluation. *arXiv preprint arXiv:2312.14867*, 2023. 2, 8, 9, 10
- [21] M. Ku, T. Li, K. Zhang, Y. Lu, X. Fu, W. Zhuang, and W. Chen. Imagenhub: Standardizing the evaluation of conditional image generation models, 2023. 2, 3
- [22] K. Lee, H. Liu, M. Ryu, O. Watkins, Y. Du, C. Boutilier, P. Abbeel, M. Ghavamzadeh, and S. S. Gu. Aligning text-to-image models using human feedback. *arXiv preprint arXiv:2302.12192*, 2023. 2
- [23] C. Li, H. Xu, J. Tian, W. Wang, M. Yan, B. Bi, J. Ye, H. Chen, G. Xu, Z. Cao, et al. mplug: Effective and efficient vision-language learning by cross-modal skip-connections. *arXiv preprint arXiv:2205.12005*, 2022. 8
- [24] J. Li, D. Li, C. Xiong, and S. Hoi. Blip: Bootstrapping language-image pre-training for unified vision-language understanding and generation. In *ICML*, 2022. 8
- [25] L. Lian, B. Li, A. Yala, and T. Darrell. Llm-grounded diffusion: Enhancing prompt understanding of text-to-image diffusion models with large language models. *arXiv preprint arXiv:2305.13655*, 2023. 2

- [26] T.-Y. Lin, M. Maire, S. Belongie, J. Hays, P. Perona, D. Ramanan, P. Dollár, and C. L. Zitnick. Microsoft coco: Common objects in context. In *Computer Vision—ECCV 2014: 13th European Conference, Zurich, Switzerland, September 6-12, 2014, Proceedings, Part V 13*, pages 740–755. Springer, 2014. 4
- [27] H. Liu, C. Li, Y. Li, and Y. J. Lee. Improved baselines with visual instruction tuning, 2023. 8
- [28] H. Liu, C. Li, Q. Wu, and Y. J. Lee. Visual instruction tuning, 2023. 8
- [29] N. Liu, S. Li, Y. Du, A. Torralba, and J. B. Tenenbaum. Compositional visual generation with composable diffusion models. In *European Conference on Computer Vision*, pages 423–439. Springer, 2022. 2
- [30] Y. Lu, X. Yang, X. Li, X. E. Wang, and W. Y. Wang. Llmscore: Unveiling the power of large language models in text-to-image synthesis evaluation. *arXiv preprint arXiv:2305.11116*, 2023. 2, 8, 9, 10
- [31] J. P. McKenna, S. Choudhary, M. Saxon, G. P. Strimel, and A. Mouchtaris. Semantic complexity in end-to-end spoken language understanding. *arXiv preprint arXiv:2008.02858*, 2020. 2
- [32] C. Meng, Y. He, Y. Song, J. Song, J. Wu, J.-Y. Zhu, and S. Ermon. Sedit: Guided image synthesis and editing with stochastic differential equations. *arXiv preprint arXiv:2108.01073*, 2021. 2
- [33] D. Petrak, N. S. Moosavi, and I. Gurevych. Improving the numerical reasoning skills of pretrained language models. *arXiv preprint arXiv:2205.06733*, 2022. 10
- [34] V. Petsiuk, A. E. Siemenn, S. Surbehera, Z. Chin, K. Tyser, G. Hunter, A. Raghavan, Y. Hicke, B. A. Plummer, O. Kerret, et al. Human evaluation of text-to-image models on a multi-task benchmark. *arXiv preprint arXiv:2211.12112*, 2022. 2
- [35] B. A. Plummer, L. Wang, C. M. Cervantes, J. C. Caicedo, J. Hockenmaier, and S. Lazebnik. Flickr30k entities: Collecting region-to-phrase correspondences for richer image-to-sentence models, 2016. 3
- [36] D. Podell, Z. English, K. Lacey, A. Blattmann, T. Dockhorn, J. Müller, J. Penna, and R. Rombach. Sdxl: Improving latent diffusion models for high-resolution image synthesis, 2023. 4
- [37] J. W. Pratt, J. D. Gibbons, J. W. Pratt, and J. D. Gibbons. Kolmogorov-smirnov two-sample tests. *Concepts of nonparametric theory*, pages 318–344, 1981. 6
- [38] A. Radford, J. W. Kim, C. Hallacy, A. Ramesh, G. Goh, S. Agarwal, G. Sastry, A. Askell, P. Mishkin, J. Clark, et al. Learning transferable visual models from natural language supervision. In *International conference on machine learning*, pages 8748–8763. PMLR, 2021. 5, 7
- [39] A. Ramesh, M. Pavlov, G. Goh, S. Gray, C. Voss, A. Radford, M. Chen, and I. Sutskever. Zero-shot text-to-image generation. In *International Conference on Machine Learning*, pages 8821–8831. PMLR, 2021. 2
- [40] A. Ramesh, P. Dhariwal, A. Nichol, C. Chu, and M. Chen. Hierarchical text-conditional image generation with clip latents, 2022. 4
- [41] R. Rombach, A. Blattmann, D. Lorenz, P. Esser, and B. Ommer. High-resolution image synthesis with latent diffusion models. In *Proceedings of the IEEE/CVF Conference on Computer Vision and Pattern Recognition (CVPR)*, pages 10684–10695, June 2022. 4
- [42] C. Saharia, W. Chan, S. Saxena, L. Li, J. Whang, E. L. Denton, K. Ghasemipour, R. Gontijo Lopes, B. Karagol Ayan, T. Salimans, et al. Photorealistic text-to-image diffusion models with deep language understanding. *Advances in Neural Information Processing Systems*, 35: 36479–36494, 2022. 2, 3
- [43] T. Salimans, I. Goodfellow, W. Zaremba, V. Cheung, A. Radford, and X. Chen. Improved techniques for training gans. *Advances in neural information processing systems*, 29, 2016. 2

- [44] M. Saxon and W. Y. Wang. Multilingual conceptual coverage in text-to-image models. In A. Rogers, J. Boyd-Graber, and N. Okazaki, editors, *Proceedings of the 61st Annual Meeting of the Association for Computational Linguistics (Volume 1: Long Papers)*, pages 4831–4848, Toronto, Canada, July 2023. Association for Computational Linguistics. doi: 10.18653/v1/2023.acl-long.266. URL <https://aclanthology.org/2023.acl-long.266>. 3
- [45] M. Saxon, X. Wang, W. Xu, and W. Y. Wang. Peco: Examining single sentence label leakage in natural language inference datasets through progressive evaluation of cluster outliers. In *Proceedings of the 17th Conference of the European Chapter of the Association for Computational Linguistics*, pages 3053–3066, 2023. 2
- [46] M. Saxon, Y. Luo, S. Levy, C. Baral, Y. Yang, and W. Y. Wang. Lost in translation? translation errors and challenges for fair assessment of text-to-image models on multilingual concepts. *arXiv preprint arXiv:2403.11092*, 2024. 3
- [47] C. Spearman. The proof and measurement of association between two things. *The American Journal of Psychology*, 15(1):72–101, 1904. ISSN 00029556. URL <http://www.jstor.org/stable/1412159>. 2, 6
- [48] A. Thawani, J. Pujara, and F. Ilievski. Numeracy enhances the literacy of language models. In M.-F. Moens, X. Huang, L. Specia, and S. W.-t. Yih, editors, *Proceedings of the 2021 Conference on Empirical Methods in Natural Language Processing*, pages 6960–6967, Online and Punta Cana, Dominican Republic, Nov. 2021. Association for Computational Linguistics. doi: 10.18653/v1/2021.emnlp-main.557. URL <https://aclanthology.org/2021.emnlp-main.557>. 10
- [49] H. Touvron, T. Lavril, G. Izacard, X. Martinet, M.-A. Lachaux, T. Lacroix, B. Rozière, N. Goyal, E. Hambro, F. Azhar, A. Rodriguez, A. Joulin, E. Grave, and G. Lample. Llama: Open and efficient foundation language models. *arXiv preprint arXiv:2302.13971*, 2023. 8
- [50] K. Valmeekam, A. Olmo, S. Sreedharan, and S. Kambhampati. Large language models still can’t plan (a benchmark for llms on planning and reasoning about change). *arXiv preprint arXiv:2206.10498*, 2022. 10
- [51] S. Wu, H. Fei, H. Zhang, and T.-S. Chua. Imagine that! abstract-to-intricate text-to-image synthesis with scene graph hallucination diffusion. *Advances in Neural Information Processing Systems*, 36, 2024. 2
- [52] M. Yarom, Y. Bitton, S. Changpinyo, R. Aharoni, J. Herzig, O. Lang, E. Ofek, and I. Szpektor. What you see is what you read? improving text-image alignment evaluation, 2023. 3
- [53] Q. Ye, H. Xu, G. Xu, J. Ye, M. Yan, Y. Zhou, J. Wang, A. Hu, P. Shi, Y. Shi, C. Jiang, C. Li, Y. Xu, H. Chen, J. Tian, Q. Qi, J. Zhang, and F. Huang. mplug-owl: Modularization empowers large language models with multimodality, 2023. 8
- [54] J. Yu, Y. Xu, J. Y. Koh, T. Luong, G. Baid, Z. Wang, V. Vasudevan, A. Ku, Y. Yang, B. K. Ayan, et al. Scaling autoregressive models for content-rich text-to-image generation. *arXiv preprint arXiv:2206.10789*, 2(3):5, 2022. 3, 4
- [55] J. Zakraoui, M. Saleh, S. Al-Maadeed, and J. M. Jaam. Improving text-to-image generation with object layout guidance. *Multimedia Tools and Applications*, 80(18):27423–27443, 2021. 2
- [56] Y. Zha, Y. Yang, R. Li, and Z. Hu. Alignscore: Evaluating factual consistency with a unified alignment function. *arXiv preprint arXiv:2305.16739*, 2023. 7
- [57] L. Zheng, W.-L. Chiang, Y. Sheng, S. Zhuang, Z. Wu, Y. Zhuang, Z. Lin, Z. Li, D. Li, E. P. Xing, H. Zhang, J. E. Gonzalez, and I. Stoica. Judging llm-as-a-judge with mt-bench and chatbot arena, 2023. 8
- [58] W. Zhu, X. E. Wang, P. Narayana, K. Sone, S. Basu, and W. Y. Wang. Towards understanding sample variance in visually grounded language generation: Evaluations and observations. *arXiv preprint arXiv:2010.03644*, 2020. 2

A Supplementary Details

For more information on the structure of the semantic error graphs (SEGs), we provide examples here. SEG 85 is one example with a more interesting topology than the example in Figure 1. Figure 8 has a structure including two-error edges, single-parent nodes, single-child nodes, multi-parent nodes, and multi-child nodes in the same graph, corresponding to prompt “*guy with umbrella hat sitting at a table with another person with a hat under a red umbrella.*”

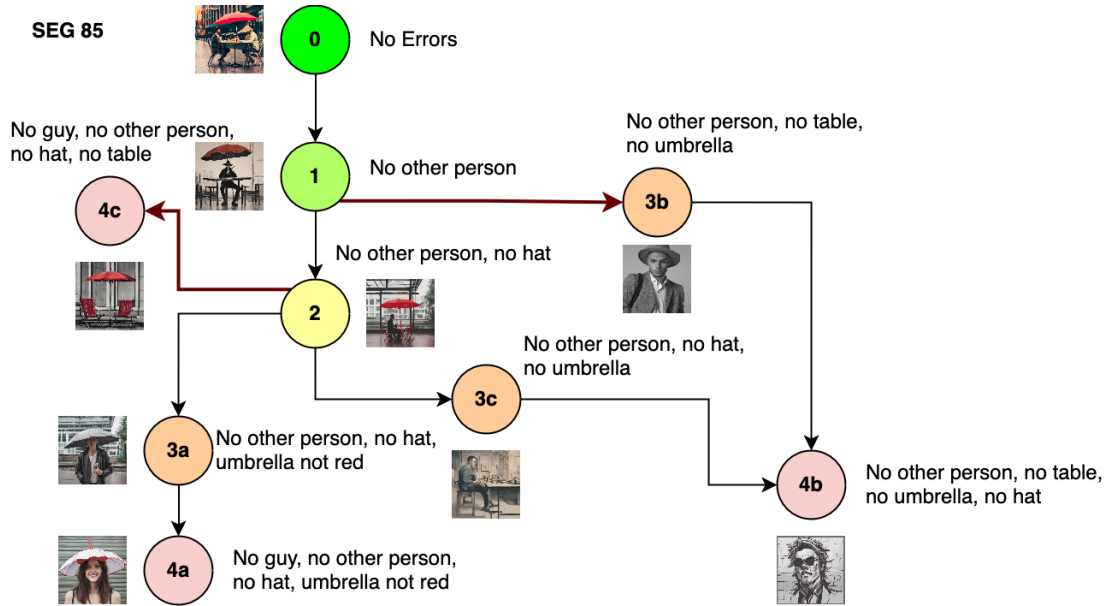


Figure 8: Example of a SEG (85) with a more complex structure. Some nodes have multiple child nodes, and some edges correspond to more than one error (**dark red**).

Figure 9 exemplifies why we choose to only score rank order *along walks* of the graph, rather than *between all pairs of nodes*. A priori there’s no reason the beach-less images should be worse than the umbrellas, yet metrics consistently rate the beach error more severe.

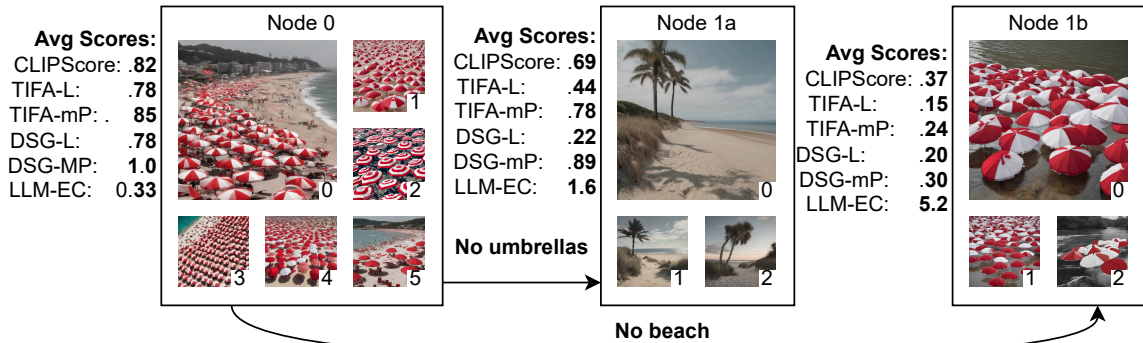


Figure 9: Examples from SEG 71 (*The beach is crowded with red and white umbrellas*). Even though both nodes 1a and 1b have the same error count (1) they systematically differ across all metrics: all metrics punish the images where the umbrellas are just in water (no beach, 1b) more than they penalize an empty beach with no umbrellas (1a).

		<i>mPLUG</i>	<i>LLaVA 1.5</i>	<i>LLaVA 1.5 (alt)</i>	<i>InstructBLIP</i>	<i>BLIP1</i>	<i>Fuyu</i>						
		DSG w/ TIFA accumulation						DSG w/ DSG accumulation					
Ord.	Avg	70.4	76.2	75	79.0	76.6	29.5	68.8	80.0	75.6	80.2	76.9	35.8
	Synth	74.6	80.1	81.6	85.1	81.6	35.4	73.5	83.8	82.1	86.1	81.7	45.5
	Nat	65.3	65.9	68.8	<i>70.7</i>	71.6	20.5	61.9	74.9	68.9	70.2	71	21.5
	Real	58.4	70.0	54.2	62	61.2	14.2	56.4	69.6	55.9	65.8	62.8	10
Sep.	Avg	78.4	83.1	80.3	84.2	80.8	63.6	75.5	82.5	80.5	84.3	80.6	66
	Synth	80.9	85.7	83.9	87.8	84.9	65.8	77.1	85.5	83.8	88.8	84.1	68.7
	Nat	71.2	80.9	76.7	81.8	73.3	68.6	70.6	75.1	77.2	81.5	75.1	71
	Real	75.1	74.5	69.4	71.9	70.8	50.3	73.1	76.8	70.6	68.9	71.4	50.8

Table 3: Comparing how using DSG vs TIFA-style accumulation for scoring each image by DSG questions impacts performance along both our metrics. The right half of this table is identical to the DSG section in Table 2, and bold, italic, and highlighting follows the same rules, except cells in the TIFA half are marked as if they were replacing the right half cells in the DSG section in Table 2.

B Supplementary Results

B.1 Comparing DSG question evaluation using DSG and TIFA score accumulation methods

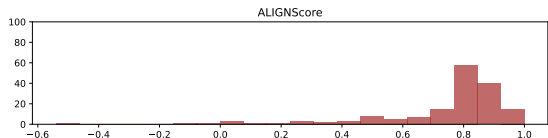
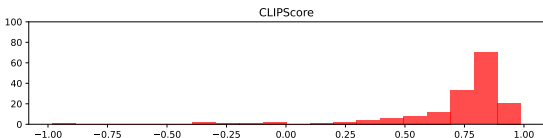
The first few steps of TIFA [13] and Davidsonian Scene Graph (DSG) [6] scoring methods are nearly identical: an LLM generates a set of requirements as questions, and a VQA system answers them. However, the two methods differ chiefly in how the answers are combined into a single image-level score. TIFA simply scores images by the correct answer rate, while DSG uses the graph structure of the requirements to build in some robustness: if an *upstream* requirement is not met (e.g., *is there a boy?* : **no**), then *downstream* requirements are all also assessed as not being met, regardless of answer. In the example provided, if the question “*is the boy’s shirt green?*” were answered **yes**, the DSG accumulation technique would still score this requirement as being not met, due to the upstream requirement, while the TIFA accumulation method would score it as being met.

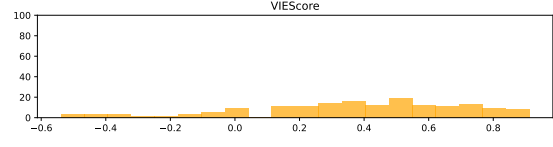
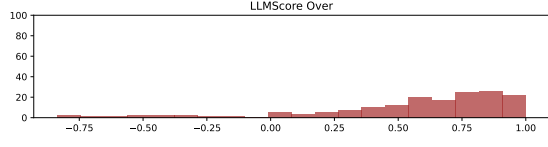
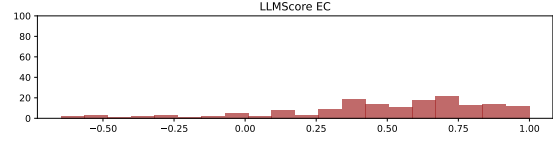
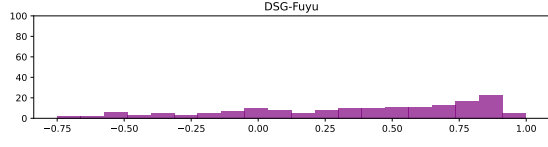
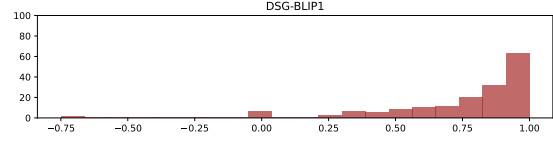
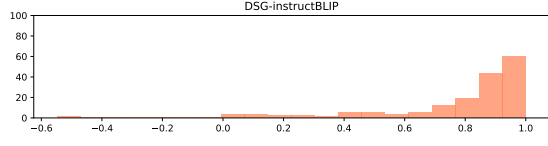
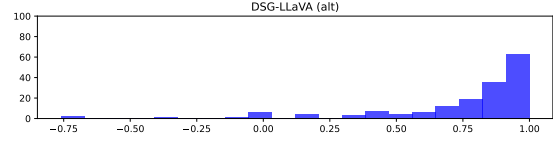
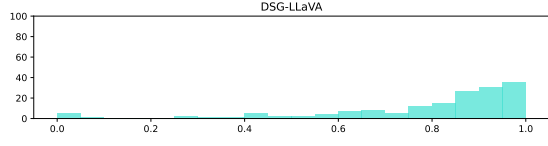
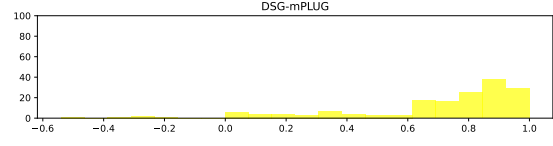
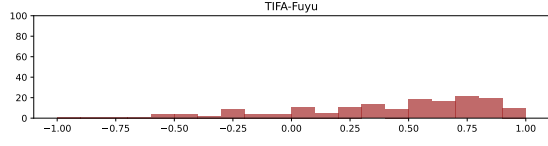
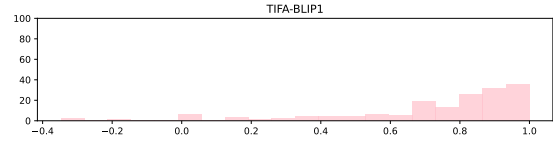
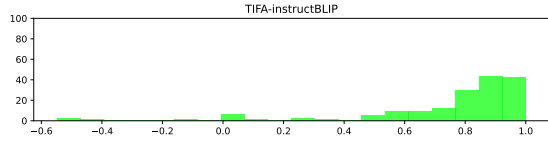
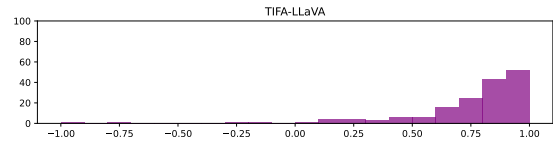
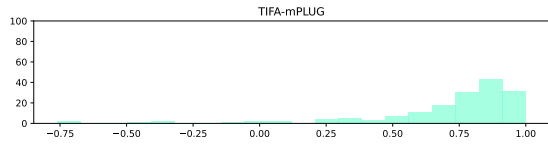
As a supplementary experiment, we compare how accumulating the DSG questions using the DSG technique compares to accumulating them with the TIFA technique in Table 3. Interestingly, the impact of this change differs between strong and weak VLMs, between ordering and separation scores, and between the easier and harder subsets. For example, switching from the DSG to TIFA-style accumulation consistently *improves ordering performance for mPLUG*, while it *worsens performance for LLaVA, InstructBLIP, and BLIP1*. For Fuyu, the weakest model, DSG-style accumulation *significantly improves performance* over TIFA. This strengthens the claim from Cho et al. [6] that using the scene graph to check requirements adds robustness; it makes a lot of sense that this robustness benefits the lowest-performing VQA systems the most.

For separation scores, TIFA accumulation improves performance of more models. In particular, TIFA accumulation pushes InstructBLIP into the top 3 for separation on the Synth subset, while no DSG metric using DSG accumulation breaks into the top 3 (red highlighted cell).

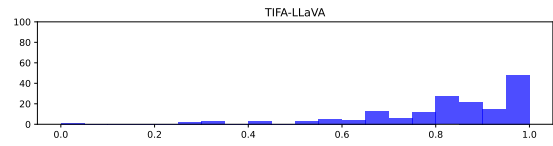
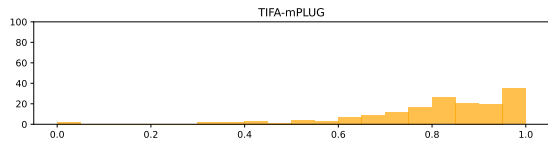
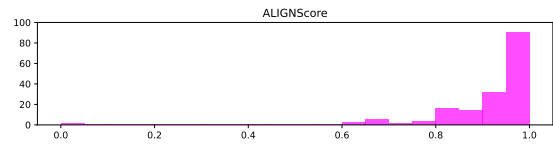
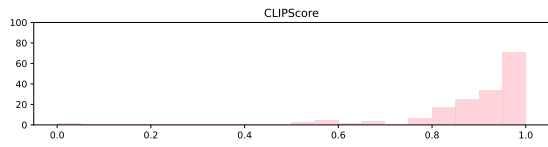
B.2 Modelwise Spearman Ordering Score Histograms

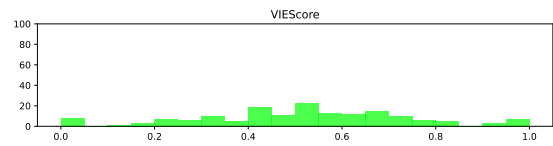
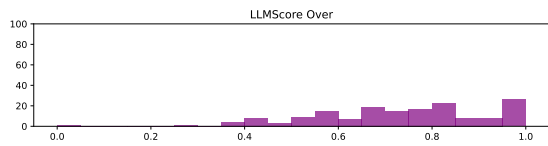
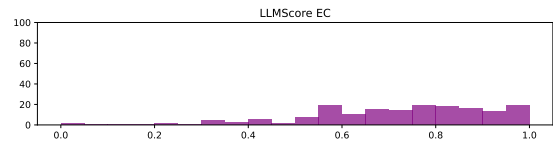
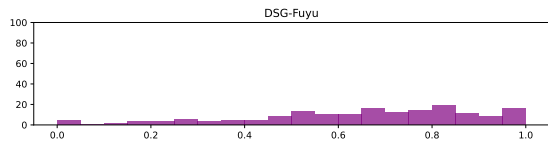
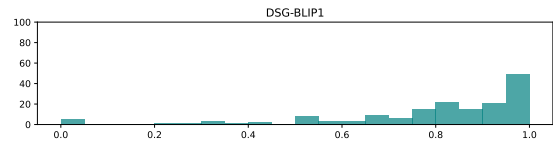
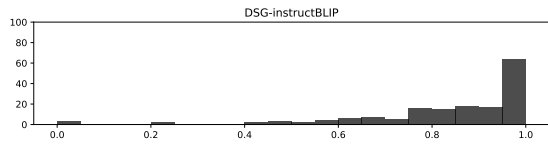
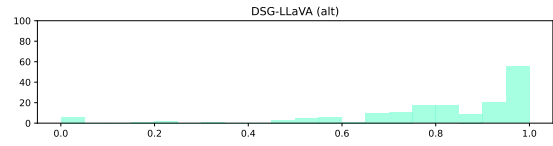
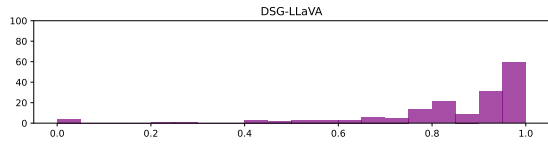
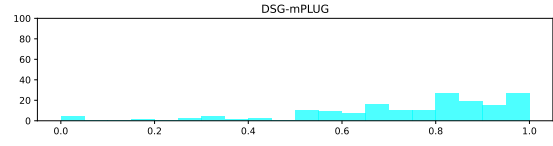
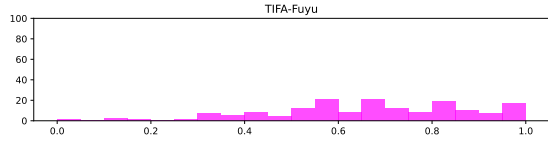
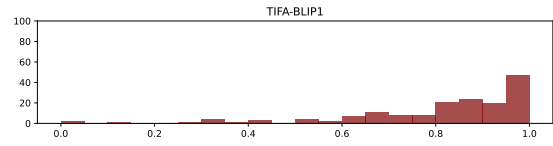
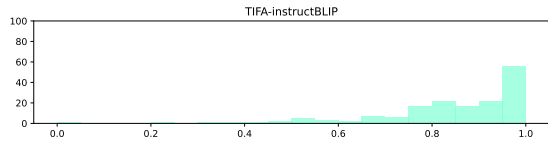
Here we provide full histograms for our Spearman Ordering and Kolmogorov–Smirnov Separation scores, across every SEG, for all metrics we assessed.



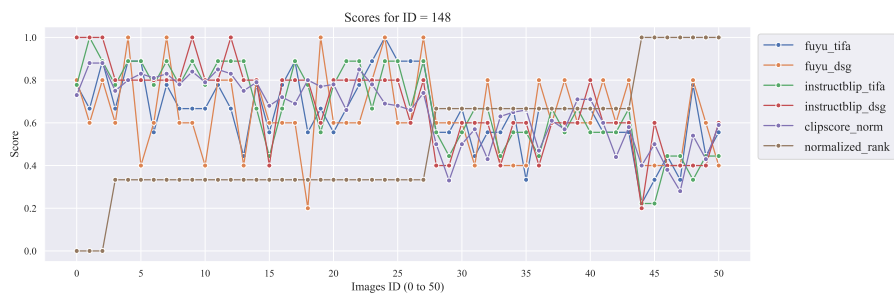
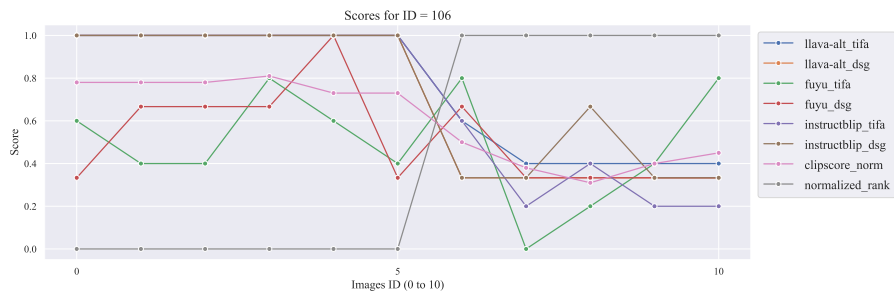
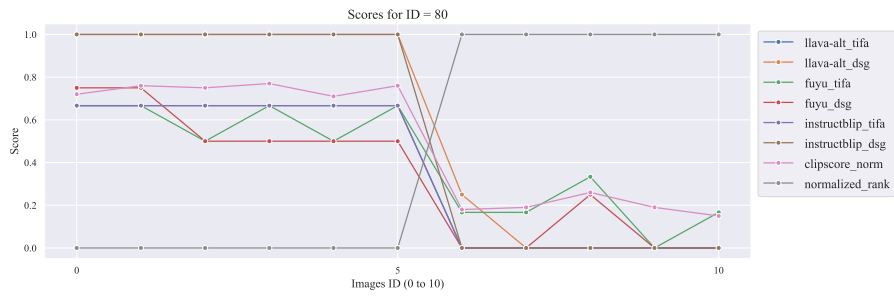
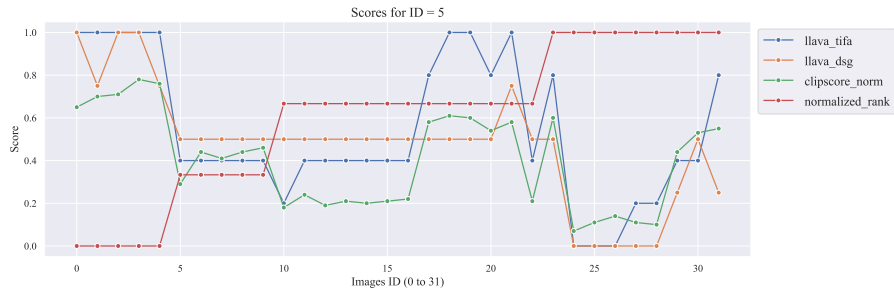


B.3 Modelwise K-S Separation Score Histograms





Here we provide line plots for a set of metrics and SEGs. Note that for `normalized_rank`, higher is worse (more errors). High-correlation is assessed when the metric lines (higher better) go down as the metric lines (higher better) go up.



C Supplementary Analysis

Figure 10 and Figure 11 show scatter plots for the Ordering (Spearman) and Separation (KS statistic) scores for every SEG between the most highly-correlated (a, b) and low-correlation (c, d) pairs of metrics under evaluation, respectively. Figure 12 and Figure 13 show all the metric-metric correlations for Ordering and Separation, respectively.

Both of these sets of figures confirm that similar underlying VLMs by-and-large “think” similarly in terms of scoring models, even over different sets of questions (TIFA and DSG). This suggests that development of overall better VLMs will generalize to many different types of VLM evaluations.

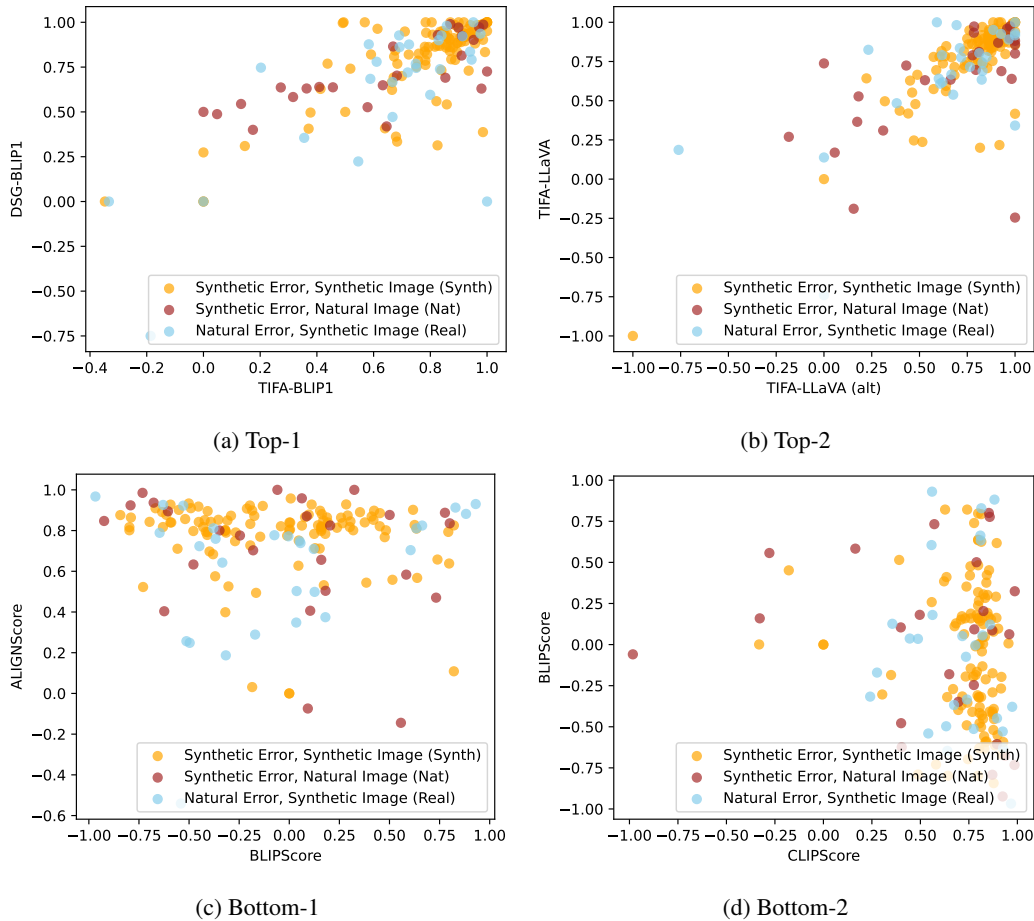


Figure 10: Scatter plots comparing the two most correlated metrics (a, b) by Spearman correlation Ordering score across the Synth, Nat, and Real populations, and the two least-correlated (c, d). Note that the two highest-correlated metrics are both QG/A metrics using the same underlying VLM (DSG and TIFA using BLIP1, (a); TIFA using LLaVA with two different system prompts, (b)).

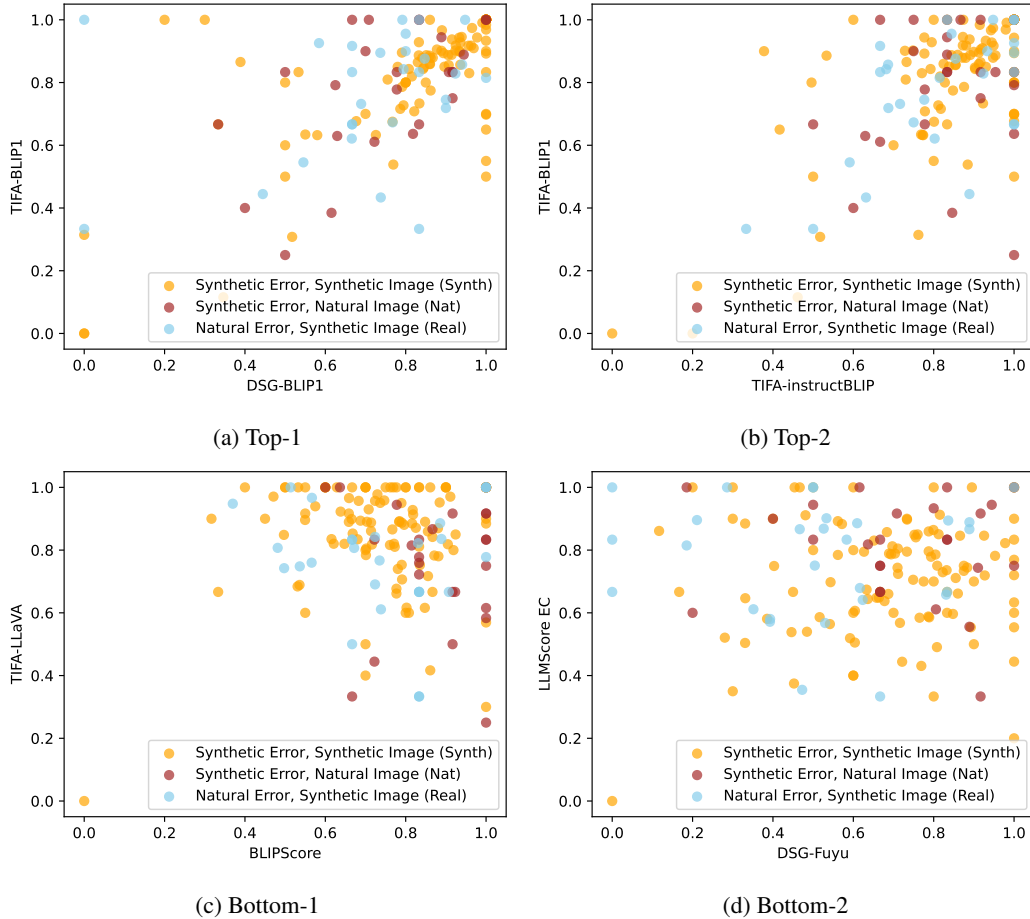
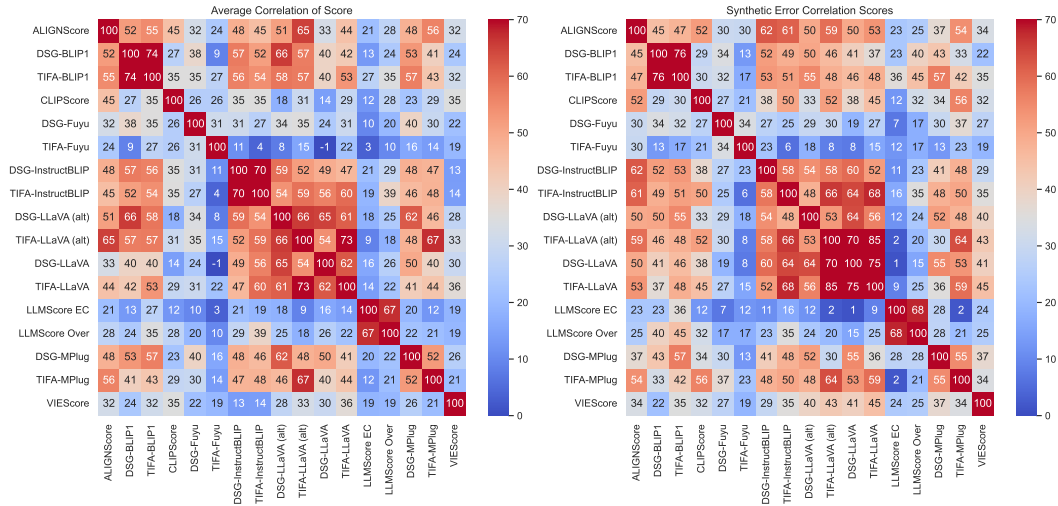
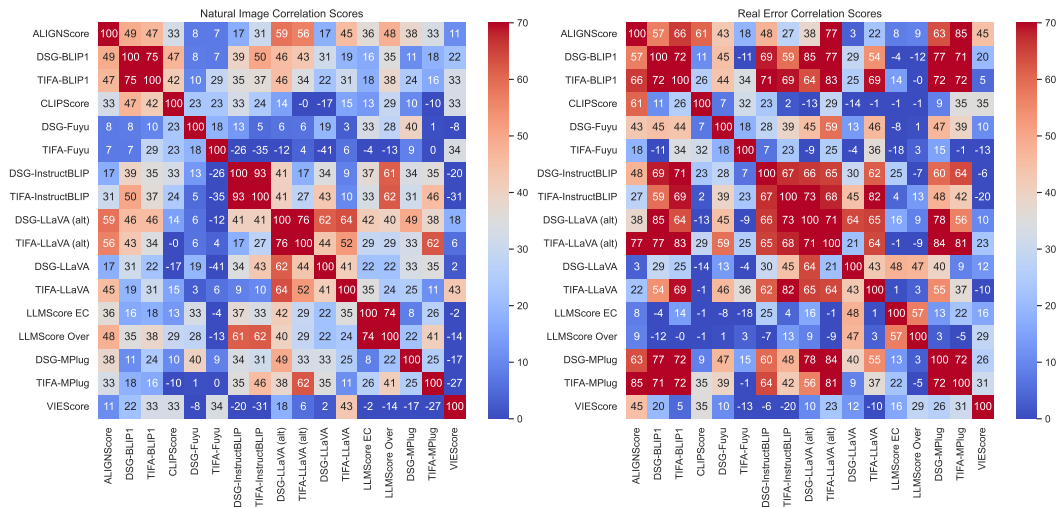


Figure 11: Scatter plots comparing the two most correlated metrics (a, b) by Kolmogorov–Smirnov Separation score across the Synth, Nat, and Real populations, and the two least-correlated (c, d). Note that the two highest-correlated metrics are both QG/A metrics using the same or related underlying VLMs (DSG and TIFA using BLIP1, (a); TIFA using BLIP1 and InstructBLIP, (b)).



(a) All SEGs

(b) Synth



(c) Nat

(d) Real SEGs only

Figure 12: Correlation between the Spearman correlation score for each prompt tree for each metric, for all SEGs (a), for the synthetic error SEGs (b), for the natural image/synthetic error SEGs (c) and for the real error subset (d).

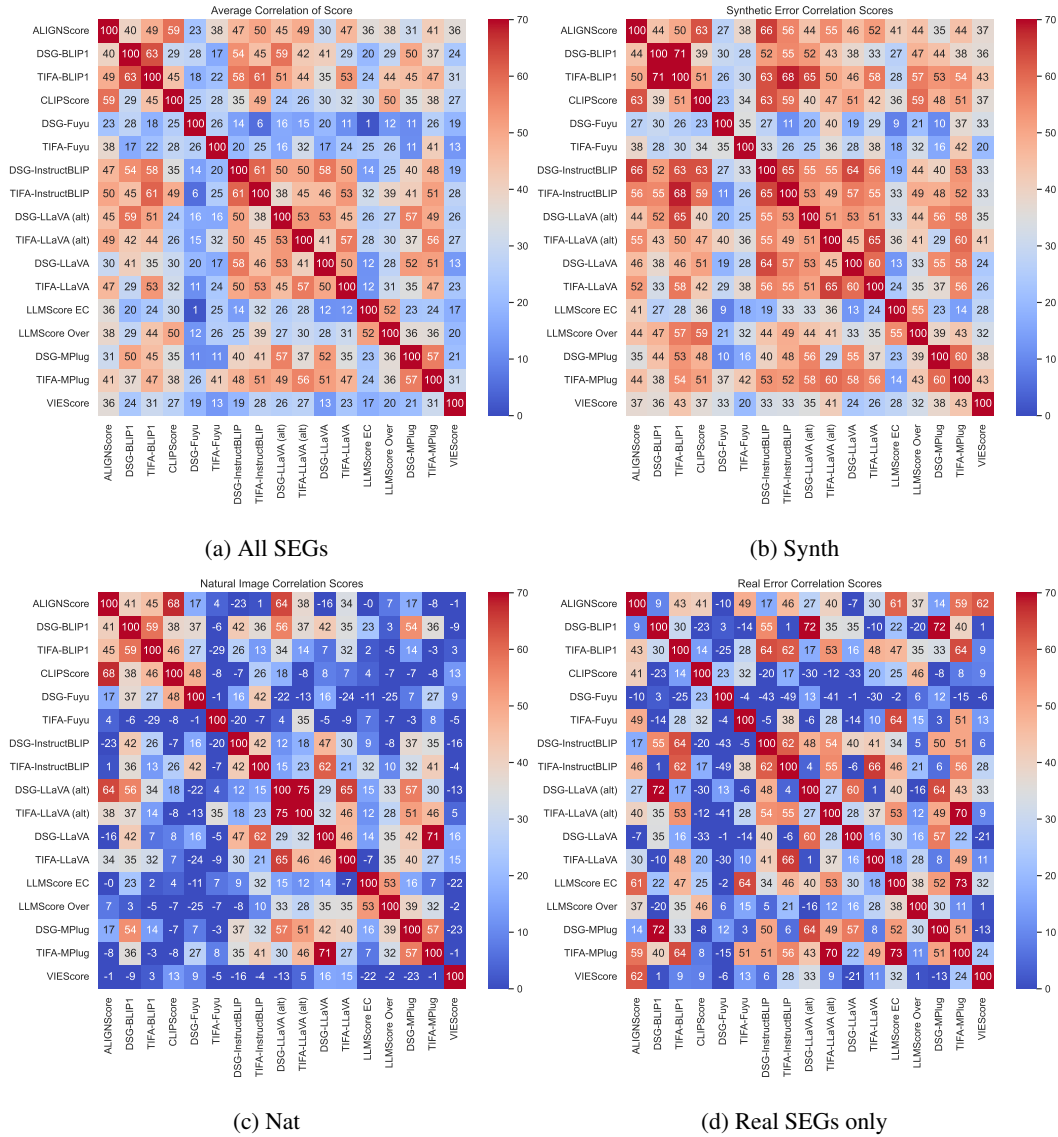


Figure 13: Correlation between the K-S Separation score for each prompt tree for each metric, for all SEGs (a), for the synthetic error SEGs (b), for the natural image/synthetic error SEGs (c) and for the real error subset (d).